TÉCNICO LISBOA

# Converting microglia into induced neural stem cells: Toward a transdifferentiation system applicable *in vitro* and *in situ*

Miguel de Araújo Godinho Henriques Pereira[a]

**Abstract**: The progressive increase in human lifespan and the increased prevalence of neurodegenerative diseases has fueled efforts to exploit the prospects of cellular programming to counteract the pathological degeneration of neural cells within the human brain. Several approaches have been investigated, including the neurotransplantation of *in vitro*-derived human cell types as well as neuronal cell fate conversion of brain-resident somatic cells *in situ*. For the latter, specifically microglia-to-neural stem cell (NSC) conversion represents an interesting alternative, combining the migratory and immunological characteristics of microglial starter cells with the merits of self-renewal and multipotent differentiation capacity exhibited by resulting NSCs. In this project, we thus applied different microglia lineage tracing systems to monitor the cell fate of iPSC-derived microglia (iPSdMiG) after Sendai virus (SeV)-mediated overexpression of the two transcription factors SOX2 and cMYC. While we were not yet successful implementing a genetic tracing system that is based on the expression of the enhanced green fluorescent protein (EGFP) under the control of the integrin subunit alpha-M (ITGAM) gene promoter (ITGAMp; gene encoding the microglial marker CD11b), due to the inability of EGFP to be efficiently transcribed and translated from the inserted construct upon differentiation of AAVS1-edited ITGAMp-EGFP-iPSCs into iPSdMiG, and the failure of a nucleofection-based editing of mature iPSdMiG to circumvent a potential differentiation-associated epigenetic silencing affecting the inserted construct, we optimized semi-continuous cell tracking using the marker Tomato Lectin. Our data overall suggest that SOX2-positive iNSC colonies, which start to appear from day 6 of conversion onwards, might indeed arise from marker-positive iPSdMiG. Thus, we next assessed whether doxycycline (DOX)-induced overexpression of SOX2 and cMYC in AAVS1-engineered iPSdMiG is able to trigger iNSC conversion, too. Although 14 day-long DOX treatment was able to induce transgene expression and promote a significant downregulation of microglial markers such as ITGAM and PU.1 in two transgenic iPSdMiG lines, NSC markers such as endoSOX2, NES and PAX6 were not significantly induced on RNA and/or protein level. As an alternative to the inducible transdifferentiation of transgenic 'convertibles', we therefore worked toward the *in vivo* conversion of primary human microglia (PhMiG). As a first step on this route, we successfully implemented a protocol for the isolation and *ex vivo* cultivation of primary microglia from human brain tissue. Subsequent studies will now need to investigate whether isolated PhMiG are principally amenable to SeV-mediated iNSC conversion. Overall, we expect this data to significantly contribute to our understanding of the potential prospects of microglia-to-iNSC conversion for future clinical therapy of neurodegenerative conditions.

**Keywords:** Neurodegenerative diseases; Regeneration; Transdifferentiation; Microglia; Neural stem cells.

## Background

Neurodegenerative diseases represent a major threat to human health, equally posing a hefty social and economic burden on the world (Ray Dorsey, E. *et al*., 2018). Partly because of the progressive extension in human lifespan, the prevalence of neurodegenerative disorders is increasing, with Alzheimer's and Parkinson's disease (PD) being the two most common human neurodegenerative pathologies observed. Affecting together more than 60 million people worldwide and more than 200,000 just in Portugal, valuable and efficient therapies for both diseases and other similar disorders are desperately needed (Ray Dorsey, E. *et al*., 2018).

Although neurodegenerative conditions can have several origins (*e.g.*, developmental, inherited or acquired) and occurrences (acute or chronic), one constant in all of them is the noticeable degeneration of neurons within the brain (Barker, R. A. et *al*., 2018). Different from other organs, the mammalian central nervous system (CNS) has a very limited capacity for self-repair though, with neurons being typically not replaced – at least not in significant numbers – upon neuronal damage or degeneration (Barker, R. A. *et al*., 2018). Accordingly, in order to resolve neurodegenerative disorders, replenishing the neuronal population affected by a disease with *ex vivo*-derived cells or exogenously promoting endogenous brain repair in patients can be considered the most promising outlines to rescue brain function (Barker, R. A. *et al*., 2018).

For the replenishment of neuronal cells in humans via *ex vivo*-derived cells, the recent technological advancements in generating and differentiating human PSCs have enabled a reliable and robust production of large numbers of disease-relevant neuronal cell types with a rather defined composition, from the patients' own somatic cells (Barker, R. A. *et al*., 2017), towards consequent direct transplantation. Yet, the restricted spread of grafted cells, the potential genomic instability of induced PSCs (iPSCs), and the risk of tumor formation (Martin, U., 2017) have precluded a faster track for the clinical application of human PSC-derived cells. Nonetheless, PSC-based therapies have turned out to be relatively safe and effective in pre-clinical experiments and meanwhile, they have entered clinical trials, especially in the last three years, with large clinical cohort studies being launched for PD across the world (Barker, R. A. *et al*., 2017).

On the other hand, a strategy to repair the brain from endogenous cells would be to exogenously stimulate neurogenesis in the adult human CNS and to recruit new-born neurons or neuroblasts from neurogenic niches to sites of neuronal injury (Barker, R. A. *et al*., 2018). However, there is a strong debate about the overall significance of these observations for the clinics, since (i) the induction of NSC proliferation might not suffice to safeguard neurogenesis but instead result in reactive astrocyte scaring (Faiz, M. *et al*., 2015), and (ii) adult neurogenesis might be species-specific

[a] *Please contact via: migueldearaujopereira@gmail.com*

and more prevalent in small brain-sized species (Paredes, M.F. *et al*., 2016), which can severely limit the potential efficacy of neurogenesis-promoting interventions.

During the last two decades, with the rise of direct cell fate conversion technology – the programming of one differentiated somatic cell into another differentiated somatic cell type without requiring a transit through a pluripotent intermediate state – and considering the characteristic properties of macroglial cells, namely their close lineage relation to neurons, their quantity (representing over half of the total brain-resident cells), their even distribution across the adult mammalian brain, and their intrinsic capacity to proliferate (Kwon, H.S. & Koh, S.H, 2020), the *in vivo* conversion of CNS-resident glial cells into functional neurons has emerged as an auspicious alternative for neural regeneration. Several studies have shown the feasibility of this process (both *in vitro* and *in vivo*), reporting that mouse brain-resident glial cells such as astrocytes, can be directly and efficiently converted into active mature neurons by the direct delivery of cell programming cues like fate-instructing transcription factors (TFs) and/or miRNAs (Flitsch, L.J. & Brüstle, O., 2019). Moreover, this direct astrocyte-to-neuron conversion strategy was also demonstrated to have clinical relevance under pathological conditions (Rivetti Di Val Cervo, P. *et al*., 2017).

Taken together, these reports underline the enormous biomedical potential of direct *in vivo* conversion of somatic cells for neural repair. In the majority of these cases, viral delivery systems were used to mediate cell fate conversion. Despite their high efficiency, viral systems might not be the most appropriate delivery systems to implement if one is looking to translate such technology into the clinics, as the high risk of insertional mutagenesis or the immune reactions potentially created by the host's own immune system against the used virus (Gurumoorthy, N. *et al*., 2022), can represent major limitations to the employability of these systems. As an alternative, non-viral systems such as nucleic acids-protecting structures, small molecules, and nanoparticles are qualified for delivering the required cell programming cues *in vivo* (Wang, S. & Huang, R., 2019). However, these non-viral systems may also pose some disadvantages, regarding low efficiency of delivery (when compared to viral systems) and low overall targetability (Dasgupta, I. & Chatterjee, A., 2021). As a substitute possibility to these viral and non-viral *in vivo* conversion factor delivery methods, an especially interesting variation of the *in vivo* transdifferentiation concept was conceived by Torper, O. *et al*. in 2013. Herein, the authors reported about the feasibility to transplant somatic cells that are already equipped to overexpress target cell type-specific TFs upon an inducing stimulus, which can then be activated after grafting to elicit an *in situ* conversion of a somatic cell into the desired cell type (Torper, O. *et al*., 2013).

In addition to the *in vivo* conversion paradigms that are based on macroglial cells as starter cells (*e.g.*, astrocyte-to-neuron), it has recently been shown that *in vivo* direct cell fate conversion can also be extended beyond germ layers, as Matsuda, T. *et al*. (2019) reported about the successful conversion of brain-resident microglia into mature neurons in the mouse brain. Microglial cells seem especially attractive and worth exploring for this neuroregenerative approaches due to their intrinsic properties, such as their role in immunosurveillance and immune response, and their plasticity and migratory potentials to quickly respond to their environment and to accumulate at lesion sites (Bachiller, S. *et al*., 2018). Notably, however, recent lines of evidence indicate that in some studies, cells that had been identified as neurons converted from TF-expressing macro- or microglial cells might have been rather experimental artifacts than to true conversion events, calling for the implementation of stringent lineage-tracing strategies in conversion experiments (Rao, Y. *et al*., 2021). Albeit this call for caution, the underlying idea of converting brain-resident cells into neurons *in vivo* to replenish degenerated cell populations could be revolutionary for the field of regenerative medicine. Yet, some limitations need first to be considered. As pointed out by Flitsch, L.J. & Brüstle, O. in 2019, as *in vivo* conversion systems continue to be perfected and their efficiencies increase, detrimental effects as the depletion of the *in vivo* target cell population can become a serious issue, especially when talking about glial cells that serve particularly vital functions. At the same time, conversion of glial cells into neurons may still restrict the yield of the technique, as neurons are postmitotic, precluding any further target cell-expansion and limiting the number of neurons in place to the number of successfully converted starter cells. Given these circumstances, *in vivo* conversion into cells with residual self-renewal capacity such as NSCs, has been envisioned as an encouraging course of action to further increase the potential of this method toward neuronal regeneration (Flitsch, L.J. & Brüstle, O., 2019).

Data from Oliver Brüstle's lab suggest the feasibility of converting iPSdMiG into iNSCs by resorting to the overexpression of two TFs, Sex determining region Y-box 2 (SOX2) and avian myelocytomatosis viral oncogene cellular homolog (cMYC; article in preparation); a transdifferentiation system based on a protocol for the conversion of adult peripheral blood cells (PBCs) into iNSCs (Sheng, C. *et al*., 2018). Although this finding holds great prospects for a potential future clinical translation, as it combines the already described characteristics of microglial starting cells with the ability of self-renewal and multipotent differentiation exhibited by the NSC target cells, several prerequisites have to be addressed in order to make this system prospectively translatable to the clinics. Thus, in this work, three investigational streams were designed at providing a collection of proof-of-principle experiments that will hopefully allow us to characterize and further develop the prospects of microglia-to-iNSC transdifferentiation. First, considering the recent publications challenging the feasibility of microglia-to-neuron conversion, we set out to implement a microglia lineage reporter system for monitoring the suggested microglia-to-iNSC cell fate transition induced by SeV-mediated overexpression of SOX2 and cMYC. Such a system would enable the specific verification of the ontogeny of arising NSCs. Addressing the former idea of Torper, O. *et al*. (2013), we secondly explored an inducible conversion system that could prospectively be applied for the *in situ* conversion of already

SOX2/cMYC-equipped iPSdMiG into iNSCs upon a stimulus. Finally, and endorsing a future *in vivo* conversion strategy targeting brain-resident primary cells, we explored whether a kit-based isolation protocol, which was optimized for the extraction of mouse primary microglia, would allow an efficient isolation and subsequent *ex vivo* propagation of microglia from human primary brain tissue.

## Materials and Methods

### IPSC culture and differentiation towards iPSdMiG

IPSCs were thawed at 37 ºC, diluted 1:10 with pre-heated DMEM/F12 medium, centrifuged at 800 rpm for 5 min and then cultured on 6-well tissue culture plates coated with vitronectin (VTN; 1:200) in StemMACS™ iPSbrew media plus 10 µM ROCK inhibitor Y-27632 (RI), only until the following medium change. Upon reaching ~90 % confluency, iPSCs were dissociated by incubation with StemPro Accutase (SPA) at 37 ºC, diluted 1:3-1:4 with DMEM/F12 medium, centrifuged at 1,300 rpm for 4 min and seeded in VTN-coated 6-well plates, in a cell concentration of $5x10^5$ cells per 6-well in iPSbrew media plus RI. For routine expansion of iPSCs, cells were washed once with 0.5 mM EDTA in DPBS, dissociated by incubation with the same solution at room temperature (RT) for ~5 min, and seeded in VTN-coated 6-well plates, in typical splitting rates of 1:2-1:6, in iPSbrew media. For assessing transgene induction levels in SOX2/cMYC-transgenic iPSC lines, iPSbrew medium was supplemented with 2 µg/ml DOX the day after cell seeding. Two days after DOX induction, iPSCs were lysed for RNA extraction. For analysis of microglia, iPSCs were differentiated into iPSdMiG by Michaela Segschneider (MS) or Mona Mathews-Ajendra (MM) according to a proprietary protocol from LIFE and BRAIN GmbH, which is detailly described elsewhere (Mathews, M. *et al.*, 2022).

### SeV-mediated overexpression of SOX2 and cMYC

For SeV-mediated iNSC conversion, wild-type (WT) iPSdMiG were retrieved from the supernatant of differentiation flasks by MS or MM. As seeding controls, a fraction of harvested cells was directly seeded in 96-well or 24-well imaging plates at a cell density of 2,679 cells/$cm^2$ and 64,935 cells/$cm^2$, respectively. For seeding, cells were centrifuged at 1,500 rpm for 5 min, resuspended in N2 medium (DMEM/F12 with HEPES, 1xN2 supplement and 2 mM Glutamax) plus 100 ng/ml recombinant human interleukin 34 (rhIL34), and distributed to Matrigel (MG)-coated (1:45) plates, as described. Remaining suspension cells were then stained for CD11b by incubation on ice with 1:50 CD11b-Phycoerythrin (PE) antibody. Afterwards, CD11b-positive cells were sorted out by Fluorescence-activated cell sorting (FACS). After FACS, two $1.5x10^5$ CD11b-purified microglia aliquots were prepared. Cells were centrifuged (described above), cell pellets were resuspended in culture medium (as described below), and aliquots were then transferred to a S2 lab. In S2, both aliquots were centrifuged at 1,500 rcf and 32 ºC for 30 min. To one cell aliquot, SeVs coding for SOX2 and cMYC (ID Pharma) were added at a multiplicity of infection of 5. After spin-infection, cells were directly plated in MG-coated 96-well or 24-well imaging plates at a cell density of 10,714 cells/$cm^2$ or 21,429 cells/$cm^2$ and 64,935 cells/$cm^2$, respectively. All plate formats were cultivated overnight (ON) in S2 under normoxic conditions (37 °C, 21 % $O_2$). Following the latter procedure, cells were detached using a cell scraper at day 1, and collected in individual tubes for centrifugation. Resulting supernatants were discarded in S2 and pellets were resuspended in the respective medium back in a S1 lab. From spin-infection on, SeV-infected cells and uninfected controls were resuspended and cultured in iNSC conversion medium (advanced DMEM/F12:Neurobasal (1:1), 1xN2, 1xB27 (without vitamin-A), 2 mM L-glutamine), 3 µM CHIR99021, 1 µM purmorphamine, 0.5 µM A83-01, 10 ng/ml human Leukemia Inhibitory Factor, 64 µg/ml L-ascorbic-acid-2-phosphate, 1 µg/ml laminin (only present in the first 10 days), and 5 µM tranylcypromine (only present in the first 10 days), while seeding controls were cultured in N2 medium plus 100 ng/ml rhIL34. Medium changes were performed every other day. At day 2, cells were stained with Tomato Lectin DyLight 594 (TL594; 10 µg/ml) for 1 hour at 37 ºC, except one well of the seeding control from each plate format serving as negative control for the staining. Re-staining with TL594 was performed at day 7 of cultivation. After incubation of TL594, wells were washed two times with DPBS before adding fresh medium to the wells. After TL594 staining at day 2, imaging plates were transferred back to S1 and maintained under hypoxic conditions (37 °C, 5 % $O_2$) up until day 14 of conversion. All S2 work was performed by Lea Berg (LB). From day 2-14, plates were daily imaged with a GE IN Cell Analyzer 2200 using the following settings: 6x6 fields of view without spaces in-between pictures, 10x objective for 24-well and 20x objective for 96-well plates, phase contrast and Cy3 channels. Images were post-processed using an image processing software. At day 14, cells were fixed in paraformaldehyde (PFA) and 24-well plates were stained for microglial and NSC markers for immunocytochemical (ICC) characterization.

### DOX-mediated conversion of iPSdMiG into iNSCs

For evaluating whether DOX-induced SOX2/cMYC overexpression from the AAVS1 safe harbor locus of human iPSdMiG would suffice to transdifferentiate iPSdMiG into iNSCs, SOX2/cMYC-transgenic iPSdMiG were seeded per MG-coated (1:60) 6 cm cell culture dish in iNSC conversion medium plus DOX with concentrations varying from 0-2 µg/ml. Cells were maintained in hypoxia and medium changes were performed every other day. At day 14 of conversion, cells of all conditions were dissociated with SPA and pelleted for cell lysis.

### Nucleofection of iPSdMiG

Nucleofection experiments were performed with a 4D-Nucleofector (Lonza) in nucleofection cuvettes using the P3 Primary Cell Line 4D-Nucleofector X-Kit L according to the manufacturer's instructions. In short, WT iPSdMiG were harvested from an iPSdMiG differentiation and were subjected to the program EN-158 or CM-158. Cells were centrifuged at 1,500 rpm for 5 min, and resuspended in nucleofection buffer consisting of kit solution and supplement, per reaction. Seeding controls were alternatively directly resuspended in STEMdiff™

APEL™ 2 (APEL) medium plus 100 ng/ml rhIL34, and subsequently seeded into one well of an uncoated or poly-L-lysine (PLL)-coated (5 µg/ml) 12-well plate. To some nucleofection reactions, 2 µg and 0.4 µg pMAX-GFP (Lonza) were added before nucleofection with the programs EN-158 or CM-158, respectively. After nucleofection, cells were seeded into one well of an uncoated or PLL-coated 12-well plate per reaction in APEL medium plus 100 ng/ml rhIL34. Cells were cultured for two days under normoxic conditions after nucleofection. For optimization of cell viability during and after nucleofection of mature iPSdMiG, cells were further exposed to three anti-apoptotic compounds, before and after nucleofection, using the program EN-158. Specifically, iPSdMiG in suspension were treated with 10 µM RI, 50 nM chroman 1 mixed with 1.5 µM Emricasan, 1:1000 polyamine supplement and 0.7 µM trans-ISRIB (altogether referred to as 'CEPT'), or 5 µM muristerone, 1 hour prior to nucleofection. Additionally, anti-apoptotic treatments were also added in the concentrations specified to the seeding medium post nucleofection. Nucleofection was otherwise performed as described. Nucleofection efficiency and cell viability were documented daily by a Personal AUtomated Lab Assistant (PAULA). At day 2 post nucleofection, flow cytometry was performed, and in which samples were measured twice, one with the presence of propidium iodide and another without this live/dead stain. Flow cytometry data were processed with FlowJo software.

### Cloning procedure, ITGAMp-EGFP-lentivirus production, and lentiviral infection of iPSdMiG

To clone pLenti-ITGAMp-EGFP vector, plasmids pAAVS1-ITGAMp-EGFP (provided by LB) and pLenti-EF1α-core-fGFP (provided by Christina Yeung) were used as templates. The ITGAMp region and the EGFP sequence within the pAAVS1-ITGAMp-EGFP were PCR-amplified with appropriate overhangs for cloning using adequate primers (described elsewhere). Gibson assembly was performed using the 2x Gibson Assembly master mix (New England Biolabs (NEB)). Thermo Fisher Scientific's plasmid DNA Miniprep and Maxiprep kits were used for DNA isolation. For production of ITGAMp-EGFP-lentivirus (LV), HEK293FT (HEK) cells were thawed and seeded on Poly-L-Ornithine-coated (5 µg/ml) 10 cm dishes in HEK medium (consisting of 1x Advanced DMEM and 2 mM L-glutamine) plus 10 % fetal calf serum (FCS). HEK cells were cultured under normoxic conditions until reaching ~70 % confluency. Afterwards, plasmid transfection and LV production were performed by LB in S2. Lipofection was performed by drop-wise addition of a mixture of OptiMEM and Lipofectamine 2000 that was beforehand incubated with 10 µg of pLenti-ITGAMp-EGFP, as well as 5 µg of each packaging plasmid, psPAX2 and pMD2G. At days 2 and 3 after lipofection, supernatants were harvested during medium change, and then were pooled and filtered through an acetate filter membrane, before ¼ volume of Lenti-X™ concentrator was added to the solution. Following 24 h-incubation at 4 °C, viral particles were concentrated by centrifugation. The virus-containing pellet was resuspended in Neurobasal medium, and LV was stored at - 80 °C until further use. For lentiviral infection, WT iPSdMiG were seeded per well of a PLL-coated 12-well plate in N2 medium with 100 ng/ml rhIL34, by MS. The next day, iPSdMiG were transferred to S2 and infected with ITGAMp-EGFP LV in a 1:50 dilution in N2 medium with rhIL34. Cells were transferred back to S1 after three medium changes. Specifically, medium was changed on days 2 and 4. On days 2, 4 and 6, GFP fluorescence of uninfected and LV-infected iPSdMiG was documented by PAULA, and on day 6, iPSdMiG were detached and collected in individual tubes, which were centrifuged at 500 rcf for 5 min. Cell pellets were resuspended in DPBS with 1:50 CD11b-PE antibody and/or 1:1000 Allophycocyanin (APC) far red fluorescent dye, which were incubated for 1 hour at RT. Antibodies/dyes were washed out following addition of DPBS and incubation at RT with vortexing once in a while. After centrifugation at 500 rcf for 5 min, cell pellets were resuspended in DPBS for flow cytometry. Data analysis was performed using FlowJo software.

### Isolation of primary human microglia

For isolating PhMiG from a brain tissue sample collected by the neurosurgical department of the University Hospital Bonn, and donated by an epileptic patient undergoing neurosurgical resection, a protocol developed by the laboratory of Annette Halle (German Center for Neurodegenerative Diseases, Bonn) for the isolation of mouse primary microglia was applied. This protocol was adapted from the manufacturer's instructions for the 'Adult Brain Dissociation Kit, mouse and rat' (Miltenyi Biotec). After cell isolation, the cell suspension was stained for the microglial marker CD11b, with 1:50 CD11b-PE being added to the cell suspension, incubating on ice and in the dark. After addition of DPBS to wash-out the antibody, cells were centrifuged. Cell pellets were resuspended in 0.1 % Bovine Serum Albumin in DPBS and 1:200 DNase and cells were passed-through a 40 µm strainer to remove cell clumps. Based on CD11b expression, microglial cells were purified using a BD FACSMelody instrument by LB. After FACS, PhMiG were manually counted and then seeded at a density of $1.6x10^4$ cells per well of a 96-well imaging plate in Adult Microglia L929 medium. Medium was changed every other day, and at day 7 of *ex vivo* culture, cells were characterized by ICC analysis.

### DNA extraction and RT-PCRs

Genomic DNA (gDNA) was extracted using the DNeasy Blood & Tissue kit (Qiagen) from frozen cell pellets according to the manufacturer's instructions. DNA concentrations were measured using a NanoDrop 2000 spectrophotometer and gDNA was stored at -80 °C. gDNA was used for genotyping of the AAVS1 locus by PCR. Primer mixes were tailored for the AAVS1 WT sequence, the AAVS1 sequence containing the transgenic construct, or both in parallel, and PCR was run on a Mastercycler X50a using the adequate cycling conditions. The same protocol was also employed for verifying the presence of the NGN2 transgenic insert within the AAVS1 locus of the corresponding genetically modified iPSC line. In addition, gDNA was also used for specifically genotyping the inserted transgene cassette by PCR. Primer mix was specific for the inserted EGFP sequence, and PCR was run on a Biometra Thermoblock using the adequate cycling conditions.

Furthermore, prior to Sanger sequencing, we attempted to amplify the genomic sequence of interest by PCR, running it on a Mastercycler X50a or on a Biometra Thermoblock, using the adequate cycling conditions. All PCRs performed relied on the Q5® High-Fidelity DNA Polymerase kit (NEB), with primer sequences being described elsewhere. All PCR products were size separated by gel electrophoresis, and their detection was accomplished by using the Bio-rad Gel Doc XR+ Imaging System. For the latter PCR, some bands of interest were excised after gel electrophoresis, with DNA being extracted using the QIAquick Gel Extraction kit (Qiagen) for consequent Sanger sequencing at Microsynth Seqlab (Bonn, Germany).

### RNA extraction, cDNA synthesis and quantitative RT-PCR (qPCR)

For RNA extraction, cells were lysed in RLT buffer plus β-mercaptoethanol (1:100). RNA was isolated using the RNeasy Mini kit (Qiagen) following the manufacturer's instructions. Isolated RNA was reverse transcribed using the qScript cDNA Synthesis kit (Quanta Biosciences). qScript PCR was run on a Biometra Thermoblock using the adequate cycling conditions. RNA and cDNA concentrations were quantified using a NanoDrop 2000 spectrophotometer. For qPCR reactions, primer sequences were specific for 18S, AAVS1-SOX2, AAVS1-cMYC, AIF1, endoSOX2, ITGAM, NES, PAX6, PU.1 or P2RY12. QPCRs were run on a Mastercycler RealPlex2 epGradient S in 96-well format using the appropriate cycling conditions and qPCR products were assessed by melting curve inspection. Cycle threshold values were normalized to the gene 18S and transformed to mean fold changes using the $2^{-\Delta\Delta Ct}$ method.

### Immunocytochemical Analyses

Cells were primarily fixed in 4 % PFA at RT. Subsequently, cells were blocked and permeabilized with 10 % FCS and 0.5 % Triton X-100 in DPBS, except for staining of PhMiG whose blocking and permeabilization was achieved with 10 % FCS in DPBS for extracellular and 10 % FCS plus 0.3 % Triton X-100 in DPBS for intracellular antibody dyes. Samples were incubated with primary antibodies ON at 4 °C in DPBS with 5 % FCS and 0.3 % Triton X-100. Primary antibodies included mouse anti-CD14 (2.5 µg/ml), APC-conjugated mouse anti-CD45 (10 µg/ml), rabbit anti-ionized calcium-binding adapter molecule 1 (IBA1; 1 µg/ml), rabbit anti-PU.1 (10 µg/ml), mouse anti-SOX2 (5 µg/ml), mouse anti-Nestin (NES; 2.5 µg/ml) and chicken anti-GFP (10 µg/ml). Following washing in DPBS with 0.3 % Triton-X, specimens were incubated with the respective secondary antibodies. Finally, cells' nuclei were counterstained with DAPI or Hoechst solution at RT. Images were acquired with a Leica DMI 6000B, and post-processed in ImageJ software.

### Statistical Analyses

All statistical analyses were performed using GraphPad Prism software and data was depicted as mean ± standard deviation of all technical replicates performed. Statistical significance was assumed for $p < 0.05$.

## Results and Discussion

### ITGAM promoter-driven EGFP expression from the human AAVS1 safe harbor locus does not efficiently label iPSdMiG

As a first proof-of-principle experiment to address the prospect translatability of a microglia-to-iNSC conversion system to the clinics, we set out to implement a genetic microglia lineage reporter approach based on the expression of a fluorescent reporter gene under the control of a cell type-specific promoter, in order to verify the ontogeny of arising NSCs from a SeV-mediated overexpression of SOX2 and cMYC. Specifically, a lineage tracing cassette that is composed of the ITGAMp followed by a sequence encoding EGFP, was introduced into the AAVS1 locus of human iPSCs. In theory, upon differentiation into microglial cells, cells derived from this transgenic iPSC line should induce expression of EGFP upon induction of ITGAM, thus marking the point when cells acquire a microglial cell identity. In the context of iNSC conversion, EGFP-positive cells should then be traced by daily imaging after infection with SeV-SOX2 and SeV-cMYC, expecting that a progressive downregulation of EGFP expression and consequent cell growth into neuroepithelial colonies could be observed in case of a successful iPSdMiG-to-iNSC conversion.

To ensure that the transgenic ITGAMp-EGFP cassette had been successfully inserted into the AAVS1 locus of iPSCs and their differentiated progeny, iPSCs and iPSdMiG were first genotyped using multiple primer combinations being either specific to the AAVS1 locus or the inserted transgene cassette. The PCR's result confirmed that while the transgenic iPSC line might have represented a mosaic line still containing a fraction of non-edited and/or heterozygous iPSCs, the derived iPSdMiG were homozygously edited in the AAVS1 locus. In addition, it was confirmed that gDNA from both, iPSCs and iPSdMiG, contained the inserted EGFP sequence. Notably, however, ICC analysis revealed that ITGAMp-EGFP-iPSdMiG did not express detectable levels of EGFP on protein level, although the microglial identity of iPSdMiG was confirmed by expression of IBA1. Thus, although an EGFP sequence could be detected by PCR amplification, EGFP was not efficiently expressed from the inserted construct, making the proposed lineage tracing system non-operational. Thus, we next aimed at verifying if the inserted EGFP sequence was devoid of point mutations precluding the transcription of a functional mRNA, which might have occurred in the process of genome editing and would have remained uncovered by the genotyping PCRs. To this end, we attempted to amplify the ITGAMp-EGFP sequence of interest of the corresponding iPSC and iPSdMiG cell lines by PCR, prior to Sanger sequencing. We first performed a gradient PCR using the ITGAMp-EGFP pDNA as template to ascertain which annealing temperature would be best suited to amplify this region of interest. From the tested annealing temperatures within the range of 55-70 ºC, all resulted in intense and clear bands with the expected size for the ITGAMp-EGFP pDNA sample. Given these favorable results, we performed a conventional PCR with 68.5 ºC as annealing temperature including the following samples: (i) ITGAMp-EGFP pDNA, serving as positive control for the specific construct under investigation, (ii) iPSC ITGAMp-EGFP and iPSdMiG ITGAMp-

EGFP, as gDNA samples of interest, (iii) ITGAMp-EGFP construct-negative, wild-type control gDNA (iPSC WT; no band expected) and (iv) a gDNA positive control derived from a quality-controlled iPSC line overexpressing the TF NGN2 from the AAVS1 locus (iPSC NGN2). Following gel electrophoresis, however, only the expected pDNA's band was detected.

Considering that the PCR even failed for the gDNA positive control, we next tested whether this included gDNA might be more sensitive to the chosen annealing temperature than the original pDNA that was used for setting up the PCR system. We thus performed a 55-70 ºC gradient PCR on iPSC NGN2 gDNA, including a single genotyping-PCR reaction with a verified annealing temperature of 63.4 ºC (see Peitz, M. *et al*., 2020 on NGN2 genotyping) as gDNA PCR control. This gradient PCR revealed that only annealing temperatures around and below 59.6 ºC would allow this sample's sequence of interest to be reasonably amplified. Moreover, the genotyping-PCR performed at 63.4 ºC resulted in the confirmation of a successfully, homozygously inserted NGN2 sequence within the AAVS1 locus of these iPSCs and thus, that the zygosity of the AAVS1 editing would not be the cause of the unseen expected band in the previous PCR.

Accordingly, we tried once more to perform a PCR with all previously tested pDNA and gDNA samples, however this time, increasing the PCR power by running a touchdown PCR, and using an annealing temperature of 56 ºC. The result conveyed that next to the previously detected, and correct, pDNA sample's band, gDNA samples of iPSdMiG ITGAMp-EGFP, iPSC WT and iPSC NGN2, now all displayed bands as well. Notably, however, most bands would not correspond to the expected sizes. Therefore, those three bands were excised from the gel, and the respective extracted DNA was sent for Sanger sequencing. According to the Sanger sequencing results, only the PCR product from the ITGAMp-EGFP pDNA contained the expected transgenic sequence, while the other gDNA samples' PCR products did not give rise to interpretable sequencing data. Thus, it was neither possible to confirm nor to exclude the occurrence of point mutations within the transgenic ITGAMp-EGFP cell lines.

## Nucleofection of iPSdMiG fails to circumvent potential differentiation-associated epigenetic silencing affecting the ITGAMp-EGFP construct

Although not able to verify the existence of point mutations within the inserted sequence, another potential phenomenon that might be precluding the expression of this reporter system was considered. In recent years, the claim that transgene expression from safe harbor loci is robust and persistent throughout differentiation has been questioned in several publications. One of these examples is in Bhagwan, J.R. *et al*., 2020, reporting that transgene expression from the AAVS1 locus of human iPSCs varies between individual iPSC clones, and is silenced during subsequent differentiation toward both hematopoietic cells and cardiomyocytes. This seems to suggest that even in the AAVS1 locus, the inserted ITGAMp-EGFP construct might have undergone epigenetic silencing in the course of iPSC-to-iPSdMiG differentiation.

A possible strategy to circumvent this issue could thus be to directly engineer the AAVS1 locus of mature iPSdMiG instead of immature iPSCs. To this end, we set out to test whether mature iPSdMiG are principally amenable to nucleofection; a prerequisite for AAVS1 engineering. Although nucleofection of PhMiG or human iPSdMiG has not yet been reported, several recent papers have addressed nucleofection of immortalized microglia-like cell lines. Accordingly, we employed the two most efficient nucleofection programs reported to date, namely programs EN-158 (Pajarskienė, J. *et al*., 2021), and CM-158, (Sui, Z. *et al*., 2007; Malikov, V. *et al*., 2022), to nucleofect human WT iPSdMiG with a small pMAX-GFP vector control plasmid. Flow cytometry analysis of iPSdMiG cells at day 2 post nucleofection (Figure 1), revealed that the program EN-158 tended to induce more cell death (24.03 % ± 7.97 > 17.68 % ± 5.38; Figure 1A) and yield a lower nucleofection efficiency (2.41 % ± 1.10 < 4.15 % ± 4.47; Figure 1B) than the program CM-158. However, for both programs, there was no difference in the percentage of GFP-positive cells within the living population whether or not pMAX-GFP plasmid was added to the nucleofection cocktail, and nucleofection efficiencies overall significantly deviated from what was previously reported in the abovementioned literature. Since the captured fluorescent live images suggested that at least for the program EN-158, GFP signal seemed to be expressed primarily in unhealthy and/or apoptotic cells, we next investigated whether the application of anti-apoptotic treatments, before and after nucleofection, could rescue this program's efficiency, preventing cell death after plasmid nucleofection. Specifically, we tested 3 treatments that were reported to counteract apoptosis, namely RI (Watanabe, K. *et al*., 2007), CEPT (Chen, Y. *et al*., 2021), and Muristerone

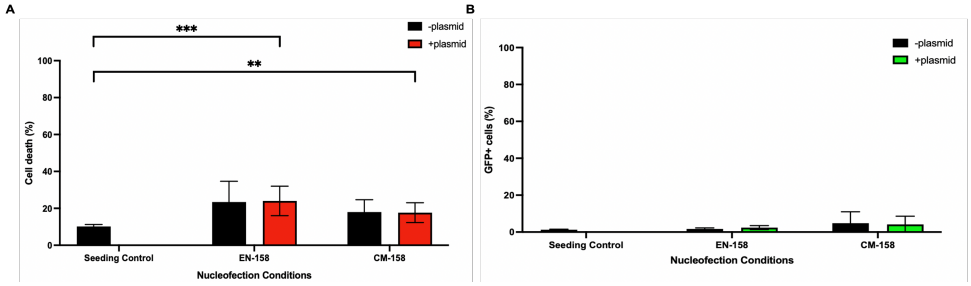


**Figure 1 – Mature iPSdMiG are not amenable to plasmid nucleofection programs employed for immortalized microglia-like cell lines. A.** Percentage of dead cells in five conditions (seeding control, as well as programs EN-158 and CM-158, each ± pMAX-GFP plasmid). N = 3 independent experiments, mean ± *SD*, ** $p < 0.01$, *** $p < 0.001$ as calculated with GraphPad Prism. **B.** Percentage of GFP-positive cells in each evaluated condition, representing nucleofection efficiency. N = 3 independent experiments, mean ± *SD*, all conditions *n.s.* as calculated with GraphPad Prism.

(Mathews, M. *et al*., 2022; Figure 2). However, none of these treatments was able to significantly reduce toxicity and thus increase nucleofection efficiency in iPSdMiG (Figures 2A & 2B).

This fact might be due to the existence of hardly any publications evaluating the effects of these drugs in iPSdMiG or microglial-like cells and that the effects of these drugs within the modulation of apoptosis were mainly evaluated in immortalized or PSC lines rather than in this cell type.

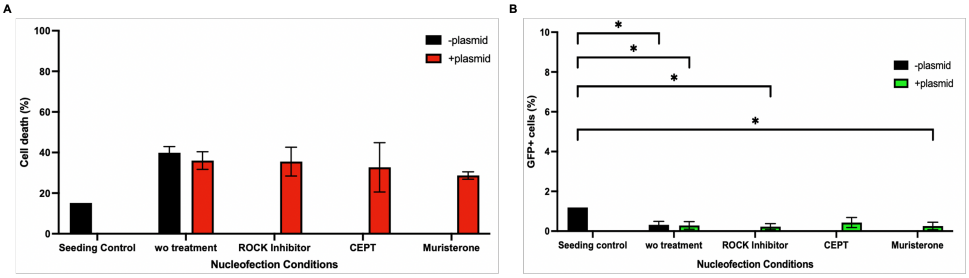


**Figure 2 – Application of anti-apoptotic treatments were unable to rescue EN-158 program's nucleofection efficiency and prevent cell death after plasmid nucleofection. A.** Percentage of dead cells in six conditions (seeding control, wo treatment (-plasmid), wo treatment (+plasmid), with RI treatment, with CEPT treatment and with Muristerone treatment). N = 3 independent experiments, mean ± *SD*, all conditions *n.s.* as calculated with GraphPad Prism. **B.** Percentage of GFP-positive cells in each evaluated condition, representing nucleofection efficiency. N = 3 independent experiments, mean ± *SD*, * $p < 0.05$ as calculated with GraphPad Prism.

Furthermore, the use of a nucleofection-based, immortalized microglial lines-optimized program in iPSdMiG can also explain this deviation from the literature, as not only it uses higher voltages than a simple electroporation technique to permeabilize the cells' nuclei, but it also relies on the premise that different cell types require different nucleofection conditions. Thus, it is safe to say that by recapitulating here the administration of anti-apoptotic drugs that were assessed to work mainly in immortalized or PSC lines, we took the first steps in testing their applicability in the modulation of apoptosis in iPSdMiG and in a nucleofection setting. However, further exploration is evidently needed as no specific nucleofection conditions nor the way the three anti-apoptotic drugs work on iPSdMiG are yet fully understood.

## Lentiviral-based strategy falls short on viability for microglia lineage tracing

Since neither the differentiation of AAVS1-edited ITGAMp-EGFP-iPSCs into iPSdMiG, nor the nucleofection-based editing of mature iPSdMiG appeared to be viable strategies for microglia lineage tracing, we next designed and cloned a lentiviral plasmid expressing EGFP under the control of ITGAMp. This construct was based on two different source plasmids, namely pAAVS1-ITGAMp-EGFP to be used as a template to amplify the transgenic insert of interest and pLenti-EF1α-core-fGFP for retrieving the lentiviral backbone. After a Sanger sequencing analysis devoid of point mutations, mismatches, or deletions within one of two produced, and examined clones, the created pLenti-ITGAMp-EGFP was subsequently used for LV production in HEK cells. To assess the functionality of the newly established LV-based reporter system, WT iPSdMiG were infected with concentrated ITGAMp-EGFP LV (performed by LB). As expected, only LV-infected cells expressed GFP 6 days after infection. Flow cytometry analysis of co-expression of CD11b, which is encoded by the endogenous ITGAM gene, and GFP, which is driven by the lentivirally inserted ITGAMp sequence, at day 6 after infection (Figure 3), revealed that while CD11b was equally expressed in non-infected and infected iPSdMiG, 7.09 % and 26.80 % of all cells expressed GFP, respectively.

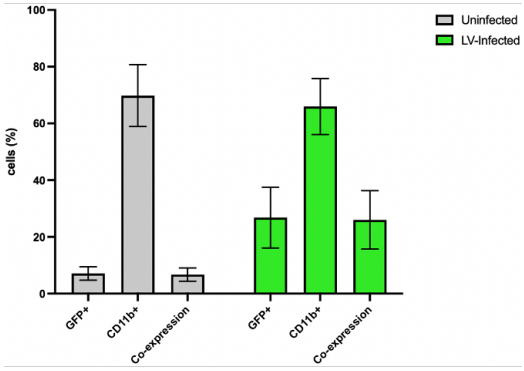


**Figure 3 – GFP and CD11b expressions display a positive linear correlation in LV-infected iPSdMiG.** Graph depicting the percentage of GFP- and/or CD11b-positive cells in two different conditions: Uninfected and LV-infected. N = 3 independent experiments, mean ± *SD*, all conditions *n.s.* as calculated with GraphPad Prism.

However, this difference was not statistically significant. Importantly though, all GFP-expressing cells seemed to co-express CD11b. Taken together, this data suggest that the produced ITGAMp-EGFP LV specifically labels CD11b-positive microglial cells. Yet, the efficiency of lentiviral infection was comparably low in our experiment. As auspicious prospects for improving efficiency of this LV-infection process, the addition of intracellular shuttling enhancers (*e.g.*, dexamethasone), intracellular barriers' inhibitors (*e.g.*, cyclosporine A and H) or a microfluidic system to the employed protocol (Gouvarchin, H.E.G. *et al*., 2020), perhaps could be considered.

Thus, and while this data seemed to emphasize a certain applicability of this system for microglia lineage tracing, given the runtime of this thesis, the explored approach was discarded, and the reasonable plausibility of this system was not confirmed. Nonetheless, future projects should carry on in evaluating this system's appropriateness for monitoring iPSdMiG-to-iNSC conversion.

## TL594-based lineage tracing system succeeds in encouraging iPSdMiG-to-iNSC conversion

An alternative to the implementation of genetic lineage tracing systems represents the use of stainable markers. Thus, we next set out to implement a staining strategy with a lectin protein obtained from *Lycopersicon esculentum*, which has affinity for specific sugar residues found on microglial cells (Villacampa, N. *et al*., 2013), to achieve the objective of monitoring iPSdMiG-to-iNSC conversion. To first determine the specificity and stability of this dye, iPSdMiG and established iNSCs were stained with TL594 (tomato lectin coupled to a fluorophore) and cultured for 14 days *in vitro* with imaging every other day. This pre-experiment confirmed the usability of this system by asserting that TL594 staining in iPSdMiG was stable for roughly 7 days, and that iNSCs were not labelled by it. After this confirmation and several rounds of optimization of the experimental setup, this was finally structured as follows: (i) Plating of freshly retrieved cells, harvested from iPSdMiG differentiation, in 96-well imaging plates (*i.e.*, serving as seeding control). (ii) Purification of iPSdMiG harvests by FACS for the microglial marker CD11b. (iii) Spin infection of FACS-purified iPSdMiG ± SeVs expressing SOX2 and cMYC (+SeV condition and uninfected control, marking day 0 of conversion). (iv) Plating of spin-infected cells at a density of 10,714 cells/cm$^2$ or 21,429 cells/cm$^2$ per well of a 96-well imaging plate or 64,935 cells/cm$^2$ per well of a 24-well imaging plate. (v) Daily imaging with IN Cell Analyzer until day 14 of conversion, with medium changes every other day and TL594 staining on days 2 and 7 of conversion. With this procedural outline, the formation of neuroepithelial-like colonies, characteristic for arising iNSCs, were observed from day 6 of conversion onwards, although, comparably stable colony placement was only noticed from around day 10 of conversion onwards. Single cells and smaller cell aggregates seemed highly dynamic and/or migratory before that time point, significantly impeding the identification of potential colony-founding cells by proximity interference. Nevertheless, based on a similar morphology and closeness to the location where iNSC colonies finally grew out, potential pairs of starting cell and arising cell aggregate were identified in images captured on consecutive days. However, for none of these observations, the identification of colony origin was indisputable. This especially applied to conditions with higher starting densities, which increased the number of potential candidates for founding cells (*e.g.*, in 24-well format). Thus, while ICC analysis at day 14 of conversion confirmed that colonies arising after SeV infection of iPSdMiG expressed the NSC marker SOX2 but neither TL594 nor the microglial marker IBA1, semi-continuous live cell imaging yielded data that encouraged, but could not ultimately manifest that TL594-positive microglia converted into iNSCs. As such, it was concluded and decided that future experiments should combine low starting cell densities of ~10,000 iPSdMiG/cm$^2$ with continuous live cell imaging so as to undeniably confirm this conversion process using this marker-based tracing system.

### Inducible microglia conversion

Since the clinical applicability of SeVs could be limited, *e.g.,* by their immunogenicity for patients (Gurumoorthy, N. *et al*., 2022), alternative strategies for the delivery of conversion-inducing TFs need to be explored. Similarly to Torper, O. *et al*. in 2013, we specifically addressed whether genomic integration of an inducible TF expression cassette could prospectively allow us to induce iNSC conversion *in situ*. The *in situ* conversion approach would be based on the transplantation of transgenic 'convertibles', being iPSdMiG already equipped with inducible transgenes (SOX2, cMYC) and thus amenable to an *in situ* conversion upon a stimulus. Analogously to our original lineage tracing strategy, lab members had previously integrated a transgenic expression cassette into the AAVS1 locus of human iPSCs, allowing inducible SOX2/cMYC expression upon DOX application. By relying on a DOX-controlled operator system, one could benefit of its straightforward usability and user-friendly layout, besides its relative safeness for *in vivo* applications – since DOX is a clinically relevant drug that can be easily administered to a patient *per os*. However, considering that our previous experiments pointed towards a potential epigenetic silencing of the AAVS1 locus upon iPSC-to-iPSdMiG differentiation, the ability of DOX to induce sufficient expression of both transgenes to trigger conversion of iPSdMiG-into-iNSCs had to be investigated. Therefore, we first assessed transgene induction levels after two day-long DOX-treatment in all available SOX2/cMYC-transgenic iPSC clones by RT-qPCR with transgene-specific primers (Figure 4). Although SOX2 and cMYC were specifically induced in the presence of DOX in all analyzed clones, expression levels varied substantially between individual clones. Future experiments need to address whether the extend of variation resulted from the zygosity of AAVS1 editing, or whether other mechanisms might have contributed to these heterogenous expression levels.

We next chose three clones with different transgene induction levels, namely c2, the clone with the highest induction of SOX2 and cMYC, c1, a clone with intermediate cMYC but comparatively low SOX2 expression levels, and c7, a clone with induction levels of SOX2 and cMYC in-between c1 and c2, for iPSdMiG differentiation. According to our hypothesis of epigenetic silencing affecting transgene expression within AAVS1 locus of human iPSdMiG, expression levels were lower in iPSdMiG after 14 days of DOX treatment than in the respective parental iPSC clone after 2 days of DOX induction. Nevertheless, comparing the induction levels of different clones to each other within one cell type, it seemed like the same trends could be observed in iPSCs and iPSdMiG.

Based on the transgene expression levels in iPSdMiG, clones c2 and c7 were chosen for further characterization. iPSdMiG from both clones were cultured in the presence or absence of DOX for 14 days in iNSC conversion medium and at the end of this period, cells were analyzed through ICC and RT-qPCR for microglial and NSC markers. The latter analysis revealed that the expression of the assessed microglial markers *ITGAM* and *PU.1*, tended to decrease upon DOX application with statistical significance. Interestingly though, NSC makers such as *endoSOX2*, *NES* and *PAX6* failed to be induced by DOX addition, and expression levels were very different from NSC marker expression in iPSdMiG-derived iNSCs converted by SeV-mediated overexpression. While DOX-induced cultures seemed to contain neuroepithelial-like colonies prior to

dissociation, ICC staining post replating further confirmed that DOX-induced cultures contained PU.1- and IBA1-expressing microglia-like cells, and were largely devoid of NES- and SOX2-expressing NSC-like cells. Altogether, these results indicate that although DOX-mediated overexpression of SOX2 and cMYC might have been able to initiate the process of conversion by enabling the decrease in expression of microglial genetic hallmarks, the expression levels of these two TFs was not enough to effectively induce iNSC lineage-instructing TFs and endogenous phenotype-provider markers, and thus, to distinctly transdifferentiate *in vitro* cultured microglia to *bona fide* iNSCs through this DOX-inducible system.

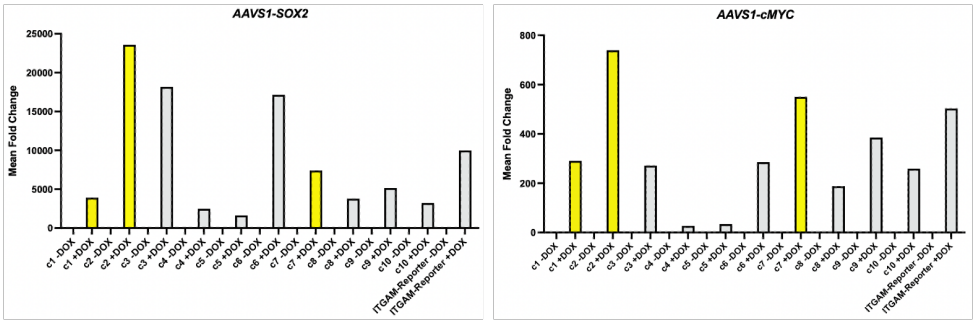


**Figure 4 – Although expression of transgenic SOX2 and cMYC is induced by DOX application, transgene induction levels after DOX-treatment are different depending on the individual iPSC clone analyzed.** Expression of the transgenic TFs SOX2 and cMYC was evaluated by RT-qPCR in iPSCs after 2 day-long culture in the presence or absence of 2.0 µg/ml DOX. Clones marked in yellow were chosen for further experiments.

The inability of this approach to work might have been due to the induction level of SOX2 and cMYC not be able to perhaps reach a given value or threshold inclined for the full conversion of cells into iNSCs, possibly owing to the DOX concentrations used. However, a more plausible explanation might be given by the potential AAVS1 locus epigenetic silencing mechanism that might be affecting the transgenic construct in iPSdMiG. As a future prospective, one can perhaps rely on other gene editing tools and use for instance, a *piggyBac*-like system to insert the DOX-inducible SOX2/cMYC construct in a random but less epigenetically influenced region of the genome. Furthermore, and given the difficulty in understanding the required levels of SOX2 and cMYC induction for *bona fide* conversion through DOX, other inducible genetic systems can perhaps also be explored, like a Cre/loxP recombinase system.

### Toward primary microglia conversion

Next to the inducible *in situ* conversion of 'convertibles', *in vivo* conversion of brain-resident, PhMiG represents an attractive route toward clinical application. The first step towards this goal would be to achieve TF-mediated PhMiG-to-iNSC conversion *ex vivo*, and a prerequisite would thus be the ability to efficiently isolate PhMiG from human brain tissue and to subsequently culture PhMiG *ex vivo* for a restricted time period. As such, we herein explored the use of an isolation protocol that is based on the 'Adult Brain Dissociation, mouse and rat' kit from Miltenyi, by processing human brain tissue. The resulting cell suspension was then FACSed for the marker CD11b, yielding ~145,000 sorted events, which equaled to ~80,000 manually counted CD11b-positive cells. Future experiments need to consolidate how this isolation efficiency relates to that of published protocols such as, Mizee, M.R. *et al.*, 2017.

After FACS, CD11b-positive cells were cultured *ex vivo* for 7 days. On day 7, iPSdMiG were seeded by Vanessa Frickel as controls for ICC analysis. Staining for the hematopoietic lineage and/or microglial markers CD14, CD45, IBA1 and PU.1 revealed that isolated cells seemed to exhibit comparable expression of CD14, CD45 and PU.1 to iPSdMiG, while IBA1 appeared to be lower in PhMiG than iPSdMiG. Moreover, expression of NSC markers SOX2 and NES was not detected in either case. Altogether, these data preliminarily indicate that microglial cells were successfully isolated by the protocol employed, and viable even after 7 days of *ex vivo* culture, with no detectable contamination of NSCs. Since this experiment could not be repeated in the runtime of this thesis due to strike-dependent personnel shortage for elective surgeries, future projects will now need to demonstrate data reproducibility, and further investigate whether isolated PhMiG are amenable to a SeV-mediated iNSC conversion *ex vivo*.

## Conclusion and Future Studies

In the present work, we aimed to address different prerequisites to make microglia-to-iNSC conversion prospectively translatable to the clinics. First, we set out to faithfully trace the ontogeny of converted iNSCs across time by lineage tracing. We found that it was not possible to employ an AAVS1-targeting, ITGAMp-driven, EGFP-based genetic lineage tracing system, as although an EGFP sequence could be detected by PCR amplification, EGFP was not being efficiently expressed from the inserted construct. Yet, we successfully re-cloned this construct for lentiviral delivery, which should now be further evaluated in the context of lineage tracing by infection of iPSdMiG and consequent induction of SeV-mediated conversion into iNSCs, as its appropriateness was emphasized by a potential positive correlation between GFP and CD11b expressions. In addition, TL594 marker-based cell tracking was explored, revealing a potential identification of iPSdMiG as founding cells of conversion-resulting iNSCs and demonstrating that iPSdMiG seem to start to be converted into iNSC-like cells from day 6 of conversion onwards. Although quite promising, follow-up experiments should still be performed to further optimize this system and to unequivocally demonstrate that iNSC colonies indeed arise from ITGAM/CD11b-expressing and/or TL594-positive microglial cells, now perhaps using a live cell imaging system. Second,

we investigated the feasibility to translate the currently employed SeV-mediated, SOX2- and cMYC-based conversion system to a DOX-inducible transgenic model, which would prospectively allow a timed conversion of SOX2/cMYC-equipped microglia into iNSCs *in situ*. Notably, we found that levels of transgenic SOX2 and cMYC induction substantially differed between iPSC clones as well as between cell types, namely in undifferentiated iPSCs and mature iPSdMiG. However, attempts to convert iPSdMiG by DOX addition similarly failed for two different clonal backgrounds, exhibiting comparably high and low induction levels. Specifically, iPSdMiG clones c2 and c7, in the presence of DOX, showed a significant decreased tendency in induction levels of specific microglial markers, but NSC makers were observed to have failed to be induced by the same drug. The inexistence of NSC-like cells was also then confirmed by ICC analysis that highlighted that this DOX system did not properly work out. Future studies should evaluate even further the applicability of this DOX-inducible system. However, if it proves ineffective in converting iPSdMiG into iNSCs, other genetic inducible systems can be explored such as the widely used Cre/loxP recombinase system. Third, we performed a preliminary experiment toward the principal possibility to convert PhMiG into iNSCs *in vivo*, in which we successfully isolated and *ex vivo*-cultivated microglial marker-expressing cells from human primary brain tissue. Although we were not yet able to test the amenability of the isolated PhMiG for iNSC conversion, we believe that pursuing this route could hold great promises for future clinical translation. Given the increasing prevalence of human brain degeneration-related diseases, the need for viable therapeutics that can not only resolve inflammation caused by degeneration of neuronal cells, but also repopulate degenerated brain areas, is undeniable. This research project thus set out to advance potentially suited technologies such as direct cell fate conversion towards translation, hoping that one day, they could revolutionize regenerative medicine.

## Declaration

This document was written and made publicly available as an institutional academic requirement and as a part of the evaluation of the MSc thesis in Biotechnology of Miguel de Araújo Godinho Henriques Pereira at Instituto Superior Técnico. The work described herein was performed at AG Brüstle, Institute of Reconstructive Neurobiology, University Bonn Medical Faculty and University Hospital Bonn (Bonn, Germany), during the period February-August 2022. The project was supervised by Lea J. Berg and Prof. Dr. Oliver Brüstle, and financially supported by the EU's Horizon 2020 program (NSC-REC) as well as the ERASMUS+ program. The thesis was co-supervised at Instituto Superior Técnico by Prof. Margarida Diogo.

## References


Bachiller, S., *et al*. Microglia in neurological diseases: a road map to brain-disease dependent-inflammatory response. (2018). *Front. in Cellul. Neurosci*., vol. 12, no. 488, pp. 1-17, doi: 10.3389/fncel.2018.00488.

Barker, R. A., *et al*. Human trials of stem cell-derived dopamine neurons for Parkinson's disease: Dawn of a new era. (2017). *Cell Stem Cell*, vol. 21, no. 5, pp. 569-573, doi: 10.1016/j.stem.2017.09.014.

Barker, R. A., *et al*. New approaches for brain repair - from rescue to reprogramming. (2018). *Nature*, vol. 557, no. 7705, pp. 329-334, doi: 10.1038/s41586-018-0087-1.

Bhagwan, J. R., *et al*. Variable expression and silencing of CRISPR-Cas9 targeted transgenes identifies the AAVS1 locus as not an entirely safe harbor. (2020). *F1000Research*, vol. 8, no. 1911, doi: 10.12688/f1000research.19894.2.

Chen, Y., *et al*. A versatile polypharmacology platform promotes cytoprotection and viability of human pluripotent and differentiated cells. (2021). Nat. Methods, vol. 18, pp. 528-541, doi: 10.1038/s41592-021-01126-2.

Dasgupta, I., & Chatterjee, A. Recent advances in miRNA delivery systems. (2021). *Methods and protocols*, vol. 4, no. 1, pp. 1-18, doi: 10.3390/mps4010010.

Faiz, M., *et al*. Adult neural stem cells from the subventricular zone give rise to reactive astrocytes in the cortex after stroke. (2015). *Cell Stem Cell*, vol. 17, no. 5, pp. 624-634, doi: 10.1016/j.stem.2015.08.002.

Flitsch, L. J. & Brüstle, O. Evolving principles underlying neural lineage conversion and their relevance for biomedical translation. (2019). *F1000Research*, vol. 8, pp. 1-17, doi: 10.12688/f1000research.18926.1.

Gouvarchin, H. E. G., *et al*. Concise review on optimized methods in production and transduction of lentiviral vectors in order to facilitate immunotherapy and gene therapy. (2020). *Biomed. Pharmacother.*, vol. 128, no. 110276, pp. 1-11, doi: 10.1016/j.biopha.2020.110276.

Gurumoorthy, N., *et al*. Non-integrating lentiviral vectors in clinical applications: A glance through. (2022). *Biomed.*, vol. 10, no. 107, pp. 1-19, doi: 10.3390/biomedicines10010107.

Kwon, H. S. & Koh, S. H. Neuroinflammation in neurodegenerative disorders: the roles of microglia and astrocytes. (2020). *Transl. Neurodeg.*, vol. 9, no. 1, pp. 1-12, doi: 10.1186/s40035-020-00221-2.

Malikov, V., *et al*. FEZ1 phosphorylation regulates HSPA8 localization and interferon-stimulated gene expression. (2022). *Cell Rep*., vol. 38, no. 7/110396, doi: 10.1016/j.celrep.2022.110396.

Martin, U. Therapeutic application of pluripotent stem cells: Challenges and risks. (2017). *Front. Med*., vol. 4, no. 229, pp. 1-8, doi: 10.3389/fmed.2017.00229.

Mathews, M., *et al*. Reenacting neuroectodermal exposure of hematopoietic progenitors enables scalable production of cryopreservable iPSC-derived human microglia. (2022). *Stem Cell Rev. Rep*., doi: 10.1007/s12015-022-10433-w.

Matsuda, T., *et al*. Pioneer factor NeuroD1 rearranges transcriptional and epigenetic profiles to execute microglia-neuron conversion. (2019). *Neuron*, vol. 101, no. 3, pp. 472-485, doi: 10.1016/j.neuron.2018.12.010.

Mizee, M. R., *et al*. Isolation of primary microglia from the human post-mortem brain: effects of ante- and post-mortem variables. (2017). *Acta Neuropathol. Commun*., vol. 5, no. 1, p. 16, doi:10.1186/s40478-017-0418-8.

Pajarskienė, J., *et al*. MicroRNA-124 acts as a positive regulator of IFN-β signaling in the lipopolysaccharide-stimulated human microglial cells. (2021). *Int. Immunopharmacol*., vol. 101, no. Pt. A 108262, doi: 10.1016/j.intimp.2021.108262.

Paredes, M. F. *et al*. Brain size and limits to adult neurogenesis. (2016). *J. of Comp. Neurol.*, vol. 524, no. 3, pp. 646-664, doi: 10.1002/cne.23896.

Peitz, M., *et al*. Protocol for the standardized generation of forward programmed cryopreservable excitatory and inhibitory forebrain neurons. (2020). *STAR Protoc.*, vol. 1, no. 1, pp. 1-15 (100038), doi: 10.1016/j.xpro.2020.100038.

Rao, Y., *et al*. NeuroD1 induces microglial apoptosis and cannot induce microglia-to-neuron cross-lineage reprogramming. (2021). *Neuron*, vol. 109, no. 24, pp. 4094-4108, doi: 10.1016/j.neuron.2021.11.008.

Ray Dorsey, E., *et al*. Global, regional, and national burden of Parkinson's disease, 1990-2016: a systematic analysis for the Global Burden of Disease Study 2016. (2018). *Lancet Neurol*., vol. 17, no. 11, pp. 939-953, doi: 10.1016/S1474-4422(18)30295-3.

Rivetti Di Val Cervo, P., *et al*. Induction of functional dopamine neurons from human astrocytes in vitro and mouse astrocytes in a Parkinson's disease model. (2017). *Nat. Biotech.*, vol. 35, no. 5, pp. 444-452, doi: 10.1038/nbt.3835.

Sheng, C., *et al*. A stably self-renewing adult blood-derived induced neural stem cell exhibiting patternability and epigenetic rejuvenation. (2018). *Nat. Com.*, vol. 9, no. 1, pp. 1-15, doi: 10.1038/s41467-018-06398-5.

Sui, Z., *et al*. Functional synergy between CD40 ligand and HIV-1 Tat contributes to inflammation: implications in HIV type 1 dementia. (2007). *J. Immunol*., vol. 178, no. 5, pp. 3226-3236, doi: 10.4049/jimmunol.178.5.3226.

Torper, O., *et al*. Generation of induced neurons via direct conversion in vivo. (2013). *Proc. Natl. Acad. Sci. U.S.A*., vol. 110, no. 17, pp. 7038-7043, doi: 10.1073/pnas.1303829110.

Villacampa, N., *et al*. Tomato lectin histochemistry for microglial visualization. (2013). *Methods Mol. Bio*., vol. 1041, pp. 261-279, doi: 10.1007/978-1-62703-520-0_23.

Wang, S. & Huang, R. Non-viral nucleic acid delivery to the central nervous system and brain tumors. (2019). *J. Gene Med*., vol. 21, no. 7, pp. 1-13, doi: 10.1002/jgm.3091.

Watanabe, K., *et al*. A ROCK inhibitor permits survival of dissociated human embryonic stem cells. (2007). *Nat. Biotechnol.*, vol. 25, no. 6, pp. 681-686, doi:10.1038/nbt1310.